# Chapter 4
# Image Presentation

## 4.1 CT Image Display

For radiologists, the most important output from a CT scanner is the image itself. As was discussed in Chapter 2, although the reconstructed images represent the linear attenuation coefficient map of the scanned object, the actual intensity scale used in CT is the Housfield unit (HU). For convenience, we replicate the mapping function below:

$$\text{CT\_number} = \frac{\mu - \mu_{\text{water}}}{\mu_{\text{water}}} \times 1000 . \tag{4.1}$$

The linear attenuation coefficient is magnified by a factor over 1000 (note the division by $\mu_{\text{water}}$). When specified in HU, air has the value of –1000 HU; water has the value of 0 HU; and bones, contrast, and metal objects have values from several hundred to several thousand HU. Because of the large dynamic range of the CT number, it is impossible to adequately visualize it without modification on a standard grayscale monitor or film. Typical display devices use eight-bit grayscales, representing 256 ($2^8$) different shades of gray. If a CT image is displayed without transformation, the original dynamic range of well over 2000 HU must be compressed by a factor of at least 8. Figure 4.1(a) shows a reconstructed image of a head phantom in which the minimum and maximum pixel intensities are –1000 HU and 1700 HU, respectively. When this dynamic range is linearly mapped to the dynamic range of the display device (0 to 255), the original grayscale is so severely compressed that little intensity variation can be visualized inside the human skull. This is clearly unacceptable. To overcome this difficulty, a CT image is typically displayed with a modified grayscale:

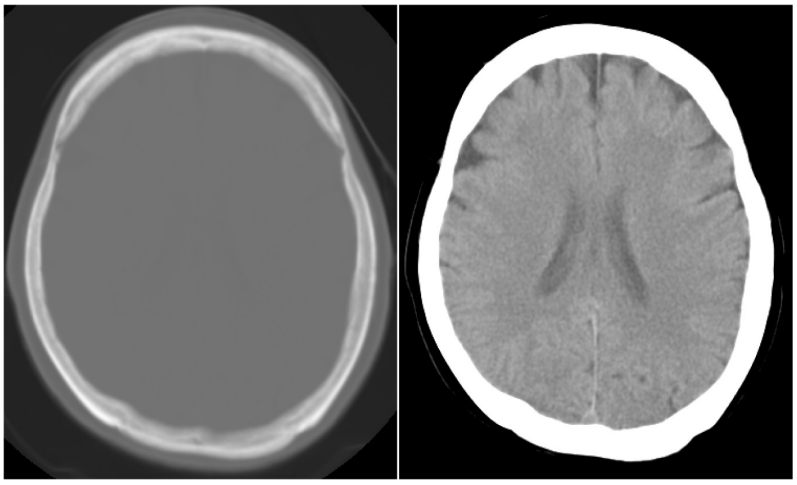

(a) (b)

**Figure 4.1** Reconstructed image of a patient head scan. (a) Image displayed with the full dynamic range of the image (2700 HU), and (b) image displayed with a WW of 100 HU and window level of 20 HU.

$$p_w(x,y)=\begin{cases}0, & p(x,y)\le L-\dfrac{W}{2}\\[2ex] \dfrac{p(x,y)-\left(L-\dfrac{W}{2}\right)}{W}I_{\max}, & L-\dfrac{W}{2}<p(x,y)\le L+\dfrac{W}{2}\\[2ex] I_{\max,} & p(x,y)>L+\dfrac{W}{2}\end{cases}. \quad (4.2)$$

Here, $L$ and $W$ are called the display window level and display window width, respectively, and $I_{\max}$ is the maximum intensity scale of the display device (for an 8-bit display device, $I_{\max} = 255$). In essence, the process maps the original intensity scale between ($L$–$W$/2, $L$+$W$/2) to the full scale of the display device, as shown in Fig. 4.2. Figure 4.1(b) shows the same head image displayed at a window width of 100 HU and a window level of 20 HU. The gray and white matter inside the brain can be clearly visualized. For convenience, the symbols "WW" and "WL" denote the display window width and window level in all figures.

Within the display window of ($L$–$W$/2, $L$+$W$/2), the display process performs a linear transformation between the reconstructed image intensity and the displayed image intensity. In many cases, however, it is desirable to perform a

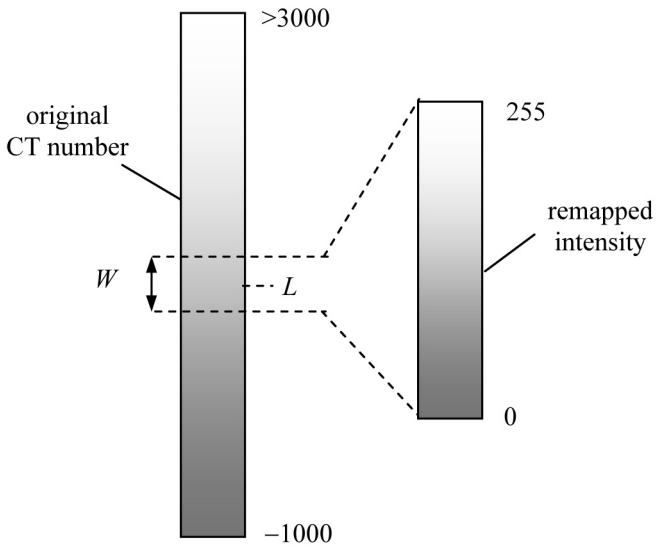


**Figure 4.2** Illustration of the display window width and window level.

nonlinear mapping between the two to change the appearance of certain features in the image. By adjusting the mapping function, these features can be enhanced or de-emphasized. In general, the mapping function can be expressed by the following equation:

$$q(x, y) = \begin{cases} G\left[p_w(x, y)\right], & t_L \le p_w(x, y) < t_H \\ p_w(x, y), & \text{otherwise} \end{cases}, \tag{4.3}$$

where $q(x, y)$ is the grayscale after the mapping, $G$ is the mapping function, $p_w(x, y)$ is the reconstructed CT value after the original window width and window level transformation, and $t_L$ and $t_H$ are parameters of the mapping function. Figure 4.3 depicts three different mapping functions: the identity function and two grayscale enhancement functions. The enhancement functions are designed so that the contrast near the CT number of 30 is increased due to the larger-than-unity slope of the two curves. Figure 4.4 shows the appearance of a CT brain image displayed with three different mapping functions. Figure 4.4(a) shows the identity mapping function in which the original reconstructed CT numbers are faithfully displayed. Although the gray and white matters in the image can be identified, their differentiation is not clearly visible. To enhance the difference between the gray and white matters in the brain, we can display the same image using the enhanced mapping functions depicted in Fig. 4.3; the results are shown in Figs. 4.4(b) and (c). However, the enhanced gray-white matter differentiation is achieved at the price of increased noise, as shown by the larger fluctuations in the uniform regions.

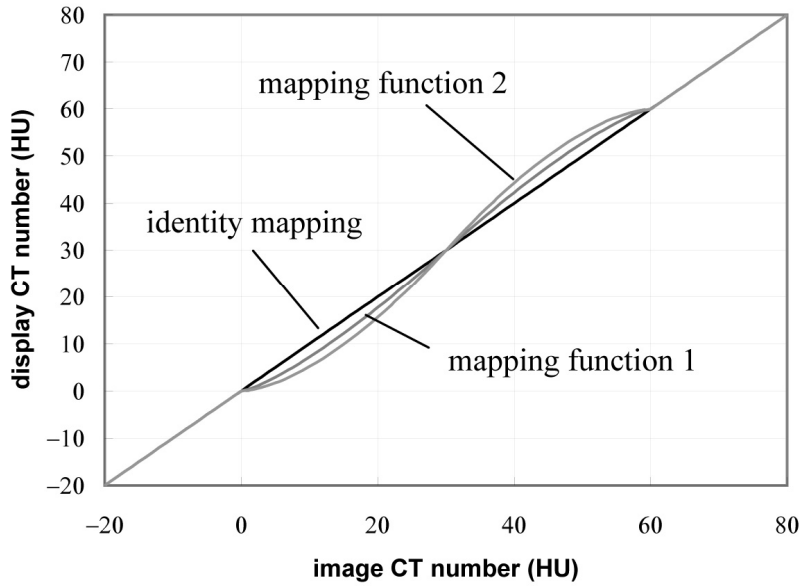


**Figure 4.3** Illustration of grayscale mapping functions.

The concept of using different mapping functions to enhance the appearance of images is not limited to CT; it was first used in x-ray radiographs to adjust the film contrast characteristic known as the gamma curve. The gamma curve describes the relationship between the x-ray exposure and the optical density of the film. By adjusting the average gradient of the gamma curve, the contrast of the imaged object can be modified. The advantage of the digital mapping function is its flexibility in defining an arbitrary function shape that is sometimes difficult to accomplish with the analog method.

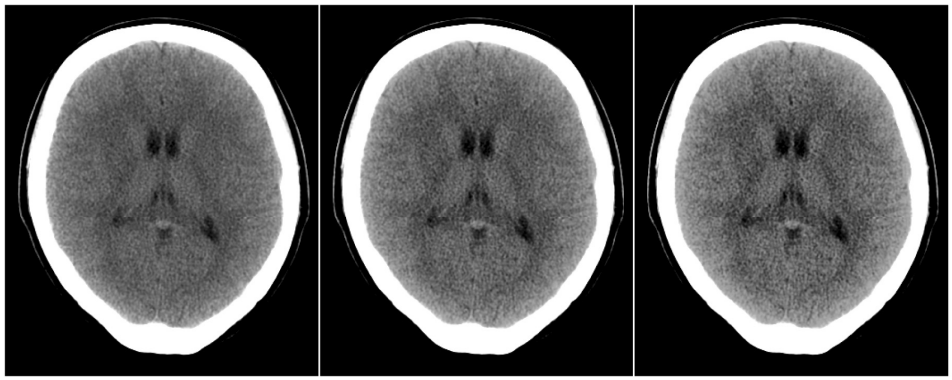

(a) (b) (c)

**Figure 4.4** Illustration of the impact of nonlinear grayscale mapping. (a) Original image, (b) mapping function 1, and (c) mapping function 2.

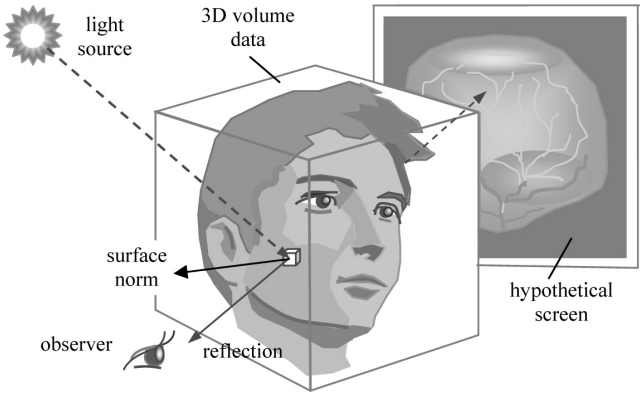


**Figure 4.24** Geometric relationships of surface rendering.

### 4.2.3 Surface rendering

Finally, we will briefly discuss the technique of surface rendering, also known as shaded surface display. The first step in surface rendering is to compute a mathematical model for the surface of the object to be rendered. The structure of the object is typically defined by a predetermined threshold. For example, a bony structure can be defined as any pixel with a reconstructed intensity above 225 HU. For a pixel to be considered part of a surface, certain connectivity requirements or criteria must be met. The surface-rendering algorithms then calculate the coordinates and the respective surface norms to describe the orientation of each point on the surface, as shown in Fig. 4.24.[8–11] For a given viewing orientation and light source, a rendered image is created with intensities proportional to the amount of light reflected by the surface toward the observer. Additional shading based on the distance of the reflective surface can also be added. Figure 4.25 shows an example of a surface-rendered ankle produced from a set of CT images.

**Figure 4.25** Surface-rendered image of a CT scan of an ankle.

## 4.3 Impact of Visualization Tools

For a long time, the primary CT viewing mode for radiologists was in the axial plane. Radiologists take pride in their ability to formulate 3D objects while viewing 2D images one slice at a time. This skill takes years of training and practice; it is remarkable to observe a radiologist analyzing CT images at a speed that is difficult for many scientists and engineers to comprehend.

With the recent technological advancements of CT, however, radiologists increasingly rely on computer visualization tools such as MIP, MPR, or VR to locate pathologies and make diagnoses. Several forces are at work to drive this change. The first is the large number of images that CT scanners currently produce for each patient. In the single-slice CT era, a typical head or body study consisted of 10 to 30 axial images, each between 5 and 10 mm in thickness. Such a study can be easily presented on a single or a few sheets of film, and radiologists seemingly spent as much time placing the films onto a lightbox as they did on the diagnosis itself. With the introduction of helical and multislice CT, the advancement in x-ray tube power, increased gantry rotation speed, and greater computer processing power, CT scanners routinely produce thin axial slices with much less than a millimeter thickness and with an acquisition time well below a patient's breath-hold. The number of axial images has increased by orders of magnitude to hundreds or even thousands for each study. Reviewing such a large number of images is an insurmountable task and can easily cause fatigue. The advanced visualization tools, on the other hand, offer the radiologist a way of viewing the entire volume in a single glance, and allows him or her to zoom in quickly on suspicious regions, instead of having to process hundreds of slices that are not related to the pathology.

The second factor is the increased ability of computers and algorithms to make the 3D volume-rendering tools fully automated, easy to use, and fast to generate. Not long ago, many institutions had a dedicated 3D laboratory to produce VR images. Radiologists had to send each study to the lab, then received the rendered images a few hours later. The 3D lab employed skilled computer scientists and technicians whose goal was to produce the best-looking 3D images. Nowadays, many of these functions can be completed at a CT console or a workstation in a matter of seconds without the involvement of a dedicated laboratory. The image generation process is quite simple and does not require expert knowledge. Although 3D laboratories still exist in many institutions, the turnaround time has been significantly reduced, and the laboratories are fully connected to CT scanners and image-viewing stations via high-speed networks. Some of these laboratories even offer services to small hospitals or clinics outside the institution.

The third driving force is the need to share information with other medical disciplines outside the radiology department. For example, CT scans are often used by surgeons who need to be informed of any abnormalities in a patient's anatomy to avoid surgical complications, or to predict the outcome of a planned procedure to repair a damaged bony structure in a patient. The 3D rendered

image becomes a communication vehicle that bridges the gap between radiologists and surgeons.

The use of advanced computer visualization tools has had a profound impact on the workflow of radiologists and the radiology department. Radiologists increasingly rely on these tools to serve as their primary reading devices. For example, when examining pathologies in extremities, reading coronal images (see Fig. 4.26) often becomes the preferred way of making a diagnosis, as opposed to reading conventional axial images. The coronal view provides a more direct visualization of the extremity structures and allows radiologist to make quicker diagnoses.

The ability of CT scanners to acquire images with isotropic spatial resolution and advanced visualization tools to generate oblique-plane images has also changed the way data acquisition is conducted. For example, CT scans were often acquired with a gantry tilt for cervical, thoracic, or lumbar vertebrae studies so that the image acquisition plane was perpendicular to the curvature of the spine, as shown by the white lines in Fig. 4.27. Scans acquired without the gantry tilt often produced suboptimal image quality because of the thick slices. Nowadays, isotropic spatial resolution can be routinely obtained, so there is little need to perform data acquisition with a gantry tilt for spine studies. Reformatted images in the oblique plane are of similar image quality compared to the images acquired directly in the oblique plane. The tilting of the CT gantry's large rotating mass during a patient scan was cumbersome and added undesirable delays to the data acquisition.

**Figure 4.26** Coronal image of an ankle.

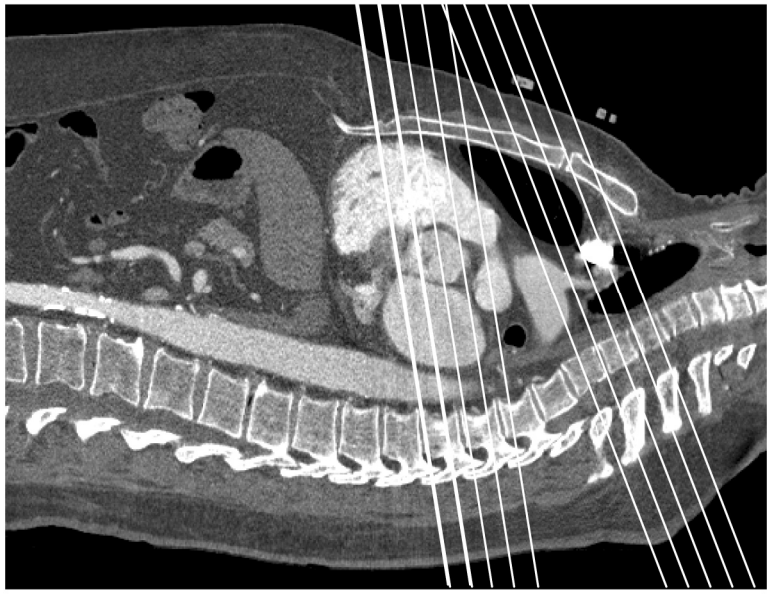

**Figure 4.27** Illustration of CT gantry tilt angle for spine scans.

One key task of a CT operator is to ensure that acquired images are of good quality. The operator must make certain that regions of suspected pathologies are properly scanned with the desired contrast uptake levels. This requires the operator to review all reconstructed images slice by slice after the data acquisition and before the patient is released. Needless to say, this is a time- and energy-consuming task, so advanced visualization tools can significantly reduce the operator's workload. For example, instead of displaying axially reconstructed images slice by slice during the data acquisition, several 3D images, such as coronal, sagittal, and VR images, can be produced and displayed simultaneously, as illustrated in Fig. 4.28. These 3D images are constantly updated as the newly reconstructed axial images become available. A quick glance at these images allows the operator to rapidly assess the CT scan quality and make decisions prior to releasing the patient.

One major challenge facing x-ray CT is the information explosion. Recent advances in CT technologies allow not only the routine production of thin slice images of isotropic spatial resolution, but also the generation of multiple image volumes over time to monitor the temporal aspect of the study. With the availability of dual-energy scanning capability (to be discussed in Chapter 12), images with functional information can be generated that add yet another dimension to the already enormous amount of data. These images need to be presented to radiologists in a clear, concise, and accurate manner to allow improved efficiency and reduced fatigue. The 3D techniques presented in this chapter are only a first step in achieving such a goal. Research and development activities in this area are progressing rapidly and are urgently needed.

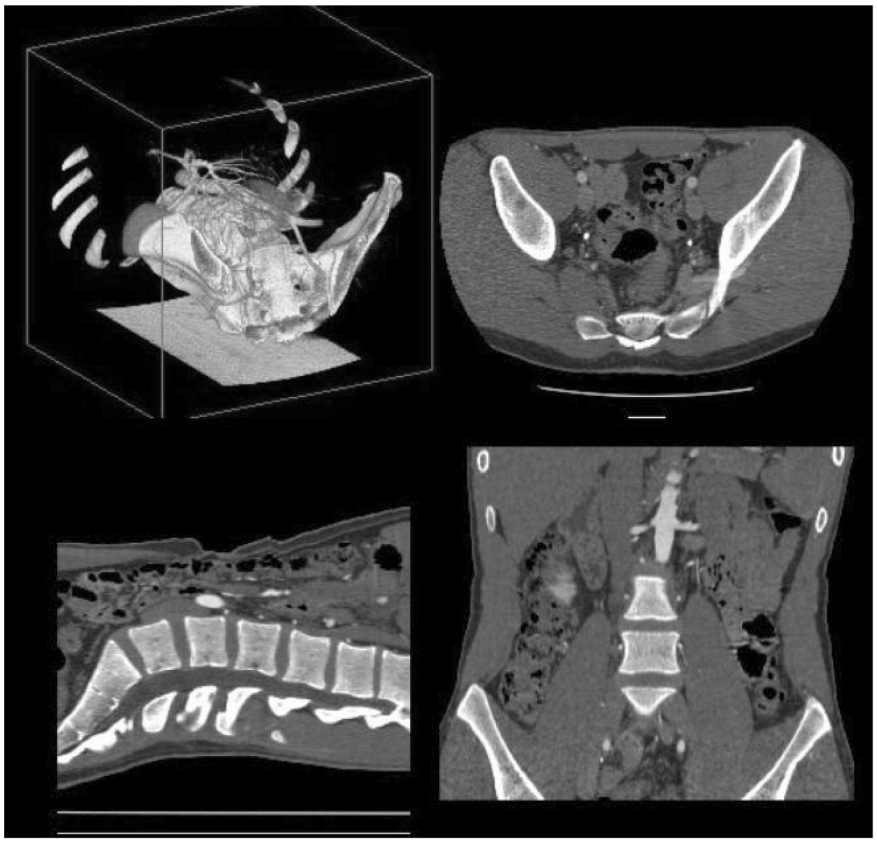

**Figure 4.28** Illustration of simultaneous displays of axial, coronal, sagittal, and VR images.

## 4.4 Problems

4-1 Images of the midbrain section are often displayed with a window width of 100 while the corresponding images of the abdomen are often displayed with a window width of 400. Assume that a brain image and an abdomen image are displayed side by side with their respective custom window widths, and that the noise levels in both images are visually identical. What is the ratio of the measured standard deviations of the original images?

4-2 In Sec. 4.1, an example was given to demonstrate the use of grayscale mapping functions to enhance image contrast [Eq. (4.3)]. For simplicity, assume that in the grayscale range of interests, the slope of the mapping function increases from 1 to 1.2. Estimate the increase in noise in the enhanced image.

4-3 Can the grayscale mapping function discussed in Sec. 4.1 [Eq. (4.3)] be discontinuous? If so, what are the potential issues?

4-4 If one designs a grayscale mapping function [Eq. (4.3)] that has a slope significantly larger than unity, what are the potential issues?

4-5 Show that, like MIP, minMIP exhibits this phenomenon: its value is dependent on the path length of the rendered object. For example, for a uniform cylindrical object, the minMIP intensity is nonuniform across the diameter of the cylinder.

4-6 Predict the amount of MIP change if the path length increases from 100 to 300 samples that are normally distributed with a mean of 0 and a standard deviation of 1. Repeat the exercise when the path length increases from 300 to 500 samples. What observation can you make with the results?

4-7 Repeat problem 4-3 with minMIP. What conclusion can you draw about the number of changes between MIP and minMIP?

4-8 A thin-slab MIP operation is performed on the reconstructed images of a uniform object with normal distributed noise. Assuming the MIP path length through the object is constant over the MIP FOV, will the standard deviation of the MIP image be higher or lower than the original reconstructed images? How will the standard deviation of the MIP image change with an increase in slab thickness?

4-9 As discussed in Sec. 4.2, one major application of MIP is the visualization of vascular structures in studies with contrast injection. Since bony structures are equally attenuating as the iodine contrast, these structures often obstruct proper viewing of the vessels. Discuss at least two approaches to solve this problem.

4-10 A patient was scanned and images were reconstructed with a 50-cm FOV. To visualize the airway structure of the lung in the A-P direction (parallel to the $y$ axis), a student wrote a program to search the minimum value along the entire image column ($y$ direction). Will the student obtain the desired result? If not, what approaches can be taken to avoid potential issues?

4-11 In a clinical application, four MIP images must be generated that correspond to projection angles of 15 deg, 30 deg, 45 deg, and 60 deg with respect to the $x$ axis. One student wrote a program that rotates the original image by −15 deg in four steps and searches the maximum intensity along each row ($x$ axis) to produce the MIP images. Another student searched the maximum intensities in the original image along straight lines of the specified angle to produce MIP images. Discuss the pros and cons of each approach.

4-12 Section 4.2 discusses issues of MIP value variation with path length due to the influence of noise. Considering the similarity between VR and